

STABILITY AND LOADS VALIDATION OF AN OCEAN CURRENT TURBINE

Henry Swales ^a
Aquantis, Inc.
Santa Barbara, CA, USA

Dave Coakley, PhD
US NSWC CD
Carderock, MD, USA

Sandeep Gupta, PhD
Helios Engineering, Inc.
Ventura, CA, USA

Stephen Way
DNV GL
Bristol, UK

^aCorresponding author: hswales@aquantistech.com

ABSTRACT

The design of a moored ocean current turbine presents many engineering challenges; among them are accurately predicting the stability and loads of the device. To validate computational loads and stability prediction tools, Aquantis Inc. designed, built, and tested a 1/25th scale model of their 'C-Plane' dual-rotor moored ocean current turbine. This effort was conducted in cooperation with the US Naval Surface Warfare Center at the David Taylor Model Basin and was funded in part under a grant awarded to Dehlsen Associates by the U.S. Department of Energy. This multi-stage testing effort included both a captured single-rotor test and a dynamic, moored test of the complete dual-rotor C-Plane. The test data is subsequently used to validate a variety of stability and loads simulations including the Navy's DCAB Code and Tidal Bladed v4.4. Specialized testing methodologies were developed for this purpose and the results are compared with computational model predictions.

This testing effort investigates many aspects of moored ocean current turbine design. The captured test was essential to characterize rotor loads and stability coefficients at various blade pitch and cone angles, as well as measure rotational stall delay and unsteady rotor loads due to upstream structure wakes. The dynamic test validated stability and loads predictions of all anticipated modes of deployment and operation, depth keeping and loads avoidance, yawed flow behavior, and various failure modes.

An extensive suite of sensors is employed on the C-Plane test model including: 6 degree-of-freedom (DOF) load cells, 6-DOF inertial measurement and heading sensors, rotor torque, rotor rpm, rotor position, static pressure/depth, tow speed, and mooring tension. These sensors provide a comprehensive understanding of the C-Plane motion and essential loads during testing. A

400Hz sample rate is utilized to accurately capture transient events. The model rotors have a high degree of controllability including ramp-up/ramp-down, counter-rotating synchronization and phase-shift, and constant tip-speed-ratio regulation.

Many challenging aspects of testing a moored ocean current turbine have been addressed in this effort, such as: very low Reynolds number scaled rotor design and fabrication, development of a mooring test rig capable of yawed flow, and simulating the motions of a dual rotor moored device. This test program has proven that the C-Plane design has a high degree of stability in a wide range of flow conditions and computational models are capable of accurately predicting C-Plane behavior.

INTRODUCTION

The Aquantis Inc. C-Plane is a dual-rotor marine turbine designed to generate up to 2.4MW per unit in the Gulf Stream and other ocean currents. Figure 1 shows the C-Plane design concept. The C-Plane is designed to operate in water depths from 100m to 400m, but is capable of being adapted to other applications such as shallow water tidal flows and extreme deep water.



FIGURE 1. C-PLANE RENDERING

In order to operate in deep ocean currents, the C-Plane utilizes a 3-point mooring system which includes two forward mooring lines to react the thrust of the rotors, and one vertical mooring line to keep the platform submerged at its minimum operating depth. As the C-Plane is a fully submerged moored device, the steady-state stability and the dynamic stability of the system are very important.

The C-Plane has been designed to have minimal roll, yaw, and pitch to keep the rotors aligned perpendicular to the flow at all times in order to maximize energy capture and minimize unsteady loading. Furthermore, the C-Plane is designed to dive as flow speed and rotor thrust increase. In the presence of a vertical shear profile of flow speed, this dive response allows the C-Plane to maintain a fairly constant flow speed at the rotor hub. The C-Plane does this passively through careful calibration of rotor thrust and net buoyancy, as well as several other design parameters affecting pitch stability. This proprietary mode of operation is known as 'passive depth control' and its validation is an essential part of this test program. Validations of the dive behavior and other aspects of C-Plane stability are achieved through a two-phase test program.

TEST APPROACH

Loads and stability validation data was gathered for the C-Plane through a comprehensive tow tank test program. The tow tank consists of an electro-hydraulic rail carriage straddling a basin of stationary fresh water. The carriage was used to propel the test apparatus through the water at specific speeds to re-create the effects of an ocean current in a controlled environment. The tow tank was used to execute two phases of testing; a captured single rotor test, and a dynamic test of the moored dual rotor platform.

The first phase of testing utilized a captured test rig (strut) to hold a single rotor and nacelle at constant yaw attitudes with respect to the flow. This phase was used to validate the rotor and nacelle hydrodynamic coefficients for a variety of configurations. Measurements were taken for the nacelle and hub without the rotor blades, and for the complete nacelle and rotor, in order to isolate the body and rotor loads.

The second phase of testing utilized a dynamic test rig to provide locations at the bottom of the basin to secure the C-Plane's three mooring lines. Measurements were taken using a comprehensive suite of sensors for a variety of flow conditions, operational modes, failure cases, and model configurations described in the Model Section.

Data was collected for a minimum of 60 seconds for each case once the position of the C-Plane reached a steady-state to provide adequate time-series data as well as case-by-case statistics. In some cases, data was also recorded during transient events such as rotor and/or flow speed acceleration/deceleration, and flow angle changes. Data was recorded at 400Hz to capture transient events such as the passage of a blade through an upstream wake. The higher sampling rate was utilized to investigate unsteady loading such as high yaw angles and passages of the rotor blades through upstream wakes.

SIMULATION APPROACH

Several computational methods were utilized to predict platform stability at various stages of C-Plane development. The simplest of these is a steady-state platform pitch and depth calculation used to quickly iterate on model design parameters such as the locations of the mooring attachments, center of gravity (CG) and center of buoyancy (CB). At the center of this calculation is a force and moment balance which takes inputs from the NREL Blade-Element-Momentum (BEM) code WT_Perf [1] and iterates on the platform depth and pitch to compute the resulting body and mooring forces and moments necessary to achieve a stable depth and pitch attitude.

Another stability simulation tool, which was used exclusively in the early stages of the C-Plane development program, is a modified version of the Navy's Cable-Body "DCAB" simulation code [2]. DCAB and its variants have an extensive history in submarine towed body development and analysis. For the C-Plane program DCAB was modified to include a separate set of coefficients for all major components of the system geometry, including the rotor(s), nacelle(s) and transverse structure. Coefficients for the rotor were obtained from a commercial, blade-element momentum (BEM) code called FlightLab. Although BEM codes have a long history in the rotorcraft and wind turbine industries, Aquantis further validated the FlightLab inputs for the C-Plane rotor through computational fluid dynamics (CFD) performed at the Applied Research Labs (ARL) at Penn State. Body hydrodynamic coefficients for the non-rotor components are generated by another Navy in-house code called BODXYZ [3].

DCAB is capable of computing time-domain simulations for a rigid representation of the C-Plane structure. It was used for analyzing the stability of conceptual and preliminary design versions of the C-Plane. In all cases it predicted that the C-Plane would be stable when operated in uniform flows and shear flows and when under large waves. Both DCAB and the steady-state

pitch/depth calculations utilize the standard submarine coordinate system utilized during testing as shown in Figure 2.

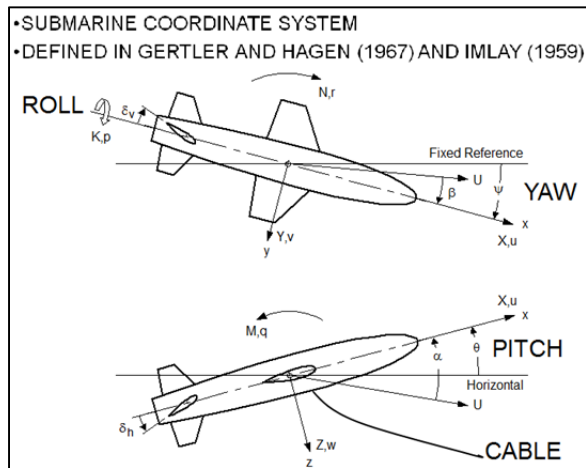


FIGURE 2. SUBMARINE COORDINATE SYSTEM

Tidal Bladed [4] from GL Garrad Hassan (now known as DNV-GL) was selected for continued internal development of a global integration model capable of providing both stability simulations and hydro-elastic loads data. The global integration model is used to model the dynamics of the C-Plane, incorporate advanced control algorithms and a full, 6 degrees of freedom (6 DOF) model of the hydrostatic drivetrain. Many of the Tidal Bladed modules are derived from Bladed, a wind turbine modeling software, with over 20 years of history.

Tidal Bladed is used to perform time-domain simulation with full hydro-elastic modeling based on multi-body dynamics. It includes models to describe the added mass effects on both the rotor and support structure. The ability to model multiple counter-rotating rotors, custom drivetrains, and incorporate an external controller makes it an ideal choice for the Aquantis C-Plane global integration model. Moorings are represented quasi-statically although there is ongoing effort to include dynamic mooring capability.

The rotor blades are modeled using 12 stations; Figure 3 shows the general blade planform used in Tidal Bladed.

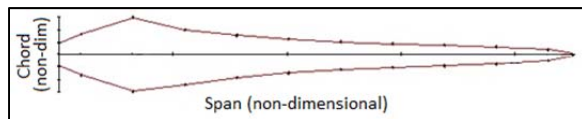


FIGURE 3. GENERAL BLADE CHORD DISTRIBUTION USED IN TIDAL BLADED SIMULAITONS

Figure 4 shows the 1/25th scale model of the Aquantis C-Plane single pod that was used for the captured test and the corresponding model in Tidal Bladed. Mass and buoyancy parameters were tuned according to the actual test article. In this first analysis, blades, nacelle and strut are assumed to be infinitely stiff.

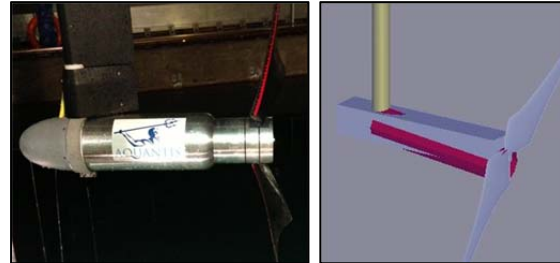


FIGURE 4. TIDAL BLADED CAPTURED MODEL

TEST FACILITY

Tow tank testing of the C-Plane was conducted the David Taylor Model Basin at the Naval Surface Warfare Center in Bethesda, Maryland. An aerial view of the facility is shown in Figure 5.



FIGURE 5. DAVID TAYLOR MODEL BASIN

The David Taylor Model Basin is one of the largest of its kind in the world, and as such enabled testing the complete mooring system of the C-Plane at a reasonable scale. Figure shows the inside of the tow basin and Carriage 2 that was used for testing.

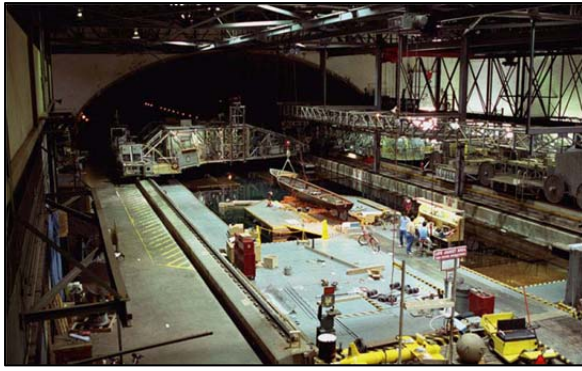


FIGURE 6. TOW CARRIAGE 2

The tow basin has the following dimensions:

- Width: 15.5m (51 ft)
- Depth: 6.7m (22 ft)
- Length: 575m (1,886 ft)

TEST APPARATUS

The test apparatus consisted of an instrumented scaled model of the C-Plane and a custom test rig to propel the model through the water. The type of test rig used was different during each phase of testing; the initial round of testing was conducted with a captured strut, and the second round of testing utilized a dynamic test rig. Sensor signals were routed via cables to a control room on the carriage. Electrical power and control signals were also passed via cable from the control room to the model. The cables are gathered into a buoyancy compensated umbilical similar in form and function to the required cabling of the full-scale device.

Captured Rig

The captured rig is composed of a 304 stainless steel pipe attached to a set of calibrated discs at the upper end for setting the yaw angle and a load cell adaptor at the lower end as shown in Figure 7.

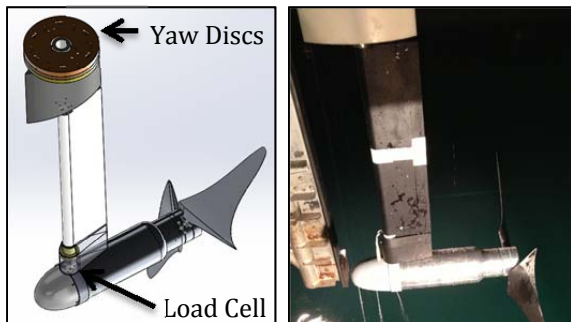


FIGURE 7. CAPTURED TEST RIG

The pipe was covered by a freely articulating Accura60 fairing to form a streamlined strut. Loads were measured using a 6-DOF load cell at

the junction of the strut and the nacelle, and by a torque sensor between the gear-motor and the rotor itself.

Dynamic Rig

The dynamic rig is primarily constructed using a 6061 aluminum alloy stage lighting truss system stiffened with Vectran cross-bracing of the vertical supports. This proved to be an extremely cost-effective and easy-to-assemble solution. The entire dynamic rig (and its submerged mooring points) is attached to and moves with the carriage as shown in Figure 8.

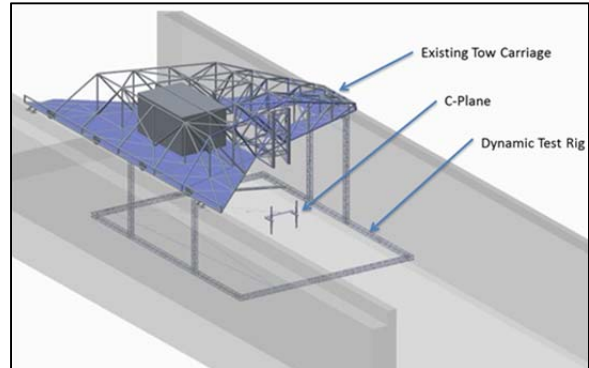


FIGURE 8. DYNAMIC TEST RIG

The forward mooring locations are mounted on a curved track which allows them to be articulated around the fixed aft mooring location. This enables setting the moorings at any angle up to 27.6 degrees with respect to the tow (flow) direction without any impact on the dimensions of the mooring system architecture.

The test rig's forward mooring lines were designed to match the scaled stiffness, wet weight, and diameter of their full-sized counterparts. The depth of the tank limited the overall length of the mooring lines to approximately $\frac{1}{2}$ of their scaled length. To account for this, specialized springs were implemented at the rig attachment point to supplement the stretch of the polyester lines themselves.

A slight oscillation was detected by divers in the aft cross-member of the dynamic rig (where the aft mooring line attaches) during check-out. This was eliminated through the application of damper plates to the underside of this member, and confirmed by the divers.

Model

The C-Plane model is composed of two identical 6061 aluminum alloy nacelles, two counter-rotating two-bladed carbon fiber rotors, a 6061 transverse structure, and Accura60 rapid prototyped buoyancy pods and fairings. The extensive use of Accura60 allowed for very

expedient development and production of complex components that also had structural requirements. Figure shows the complete model assembled with the mooring and umbilical in the basin.



FIGURE 9. C-PLANE MOORED TEST MODEL

Scaling

Froude scaling is the most appropriate scaling approach in which gravitational effects (weight and buoyancy) are major contributors to the overall platform stability. Froude scaling laws dictate the scaling factors shown in Table 1 ($\lambda=1/25^{\text{th}}$ of full-scale).

TABLE 1. SCALING FACTORS

Parameter	Scaling Factor
Mass, Volume	λ^3
Force	λ^3
Torque	λ^4
Time	$\lambda^{-0.5}$
Flow Speed	$\lambda^{0.5}$
Reynolds Number	$\lambda^{1.5}$

Due to the above Froude scaling laws and the use of a fresh water test environment, the blade chord Reynolds numbers of the $1/25^{\text{th}}$ scale model (including the rotor) is approximately $1/125^{\text{th}}$ of the full-scale values. Because of this, the full-scale rotor geometry cannot be directly scaled down. Instead, specific hydrofoils were selected for the model rotor which were designed and tested for the Reynolds number of the model rotor in the tow tank environment. The model rotor was then re-designed using these foils for the Froude scaled diameter, rotor speed, and thrust. Special consideration was made to avoid regions of flow instability such as laminar separation bubbles.

The test model was designed with a great deal of adjustability to facilitate experimentation with various configurations. The center of gravity and buoyancy are quickly adjusted by shifting the buoyancy pods and/or transverse structure (the strut which connects the two nacelles) without

affecting net buoyancy. Mooring attachments to the transverse structure are made using a set of brackets. The mooring brackets have interchangeable lengths and can be mounted at any lateral location, as well as rotated about the pitch axis to provide a great deal of adjustability. The fairing used on the transverse structure is neutrally buoyant so the model can be tested with or without the fairing without affecting net buoyancy. This adaptability made it possible to efficiently re-configure, tune, and test a wide range of model configurations providing insight into various stability drivers and generating multiple data points for simulation validation.

Instrumentation

The C-Plane model was extensively instrumented to provide a very comprehensive suite of stability and loads data. The instrumentation package included the following sensors:

- 2x 6-DOF Load Cells
- GX3 & VN100 Inertial Measurement Units
- Rotor Speed, Position, Torque
- Carriage Speed
- Depth Sensor
- Submerged & Above Water HD Video
- Tension Sensors on All Mooring Lines

The second VN100 IMU was added to provide improved directional (yaw) tracking in the test basin through the implementation of combined magnetic and inertial sensing and advanced Kalman filtering. Figure 10 shows the GX3 IMU on the foreground and the VN100 on the far side of the centrally-mounted instrumentation tray. The pressure sensor is visible as mounted under the GX3.



FIGURE 10. INERTIAL MEASUREMENT UNITS AND PRESSURE SENSOR

Sensitivity checks were performed on the pressure sensor with and without the fairing over a range of flow speeds and platform attitudes while restraining the platform at its minimum

operating depth. The pressure sensor implementation proved to be very consistent across all cases; Figure 11 shows less than 0.2ft deviation from the initial depth was measured.

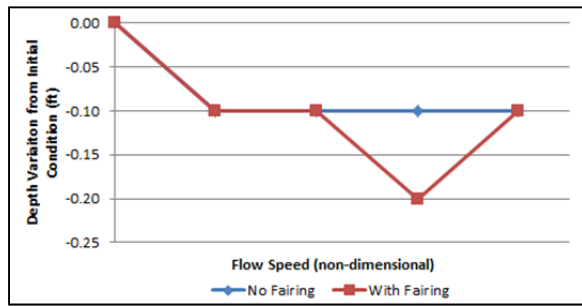


FIGURE 11. DEPTH SENSITIVITY WITH FAIRING

CAPTURED TEST

The initial captured test cases are designed to calibrate the rotor blade pitch to achieve the intended thrust at the design tip speed ratio (TSR). The model rotor is designed with boundary layer trips to minimize low Reynolds number flow instabilities, so the blade pitch must be calibrated for both the as-built rotor geometry and the boundary layer trip implementation.

Once blade pitch and boundary layer trips are finalized, the remaining test matrix explores loading over a range of rotor cone angles, yaw angles, flow speeds, and rotor speeds.

Data Processing

Figure 12 and Equation 1 show how load cell measurements are reduced to a pure rotor yaw moment for comparison with FlightLab or WT_Perf. Tidal Bladed is capable of generating loads data at the location of the load cell, enabling a direct comparison with test data.

$$Mz_0 = (Mz_r - Mz_n) - [(Fy_r - Fy_n) * XposLoadCell] \quad (1)$$

Where,

Mz_0 = Rotor Yaw Moment

Mz_r = Platform Yaw Moment (Rotor & Nacelle)

Mz_n = Nacelle Only Yaw Moment

Fy_r = Platform Side Force (Rotor & Nacelle)

Fy_n = Nacelle Only Side Force

$Xpos$ Load Cell = Longitudinal Distance from Load Cell to Rotor Reference Point

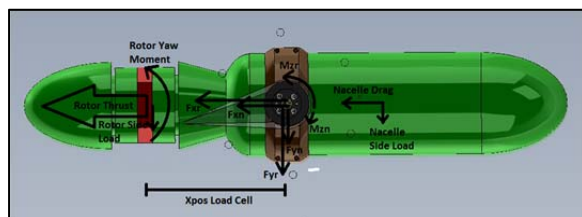


FIGURE 12. FREE-BODY DIAGRAM OF CAPTURED TEST MODEL

Boundary Layer Trip Calibration

Matching the trip geometry used in the 2D hydrofoil performance testing was desired to attain the best match between predicted and measured loads. Figure 13 shows the as-built trip used on the rotor blades during tow tank testing. One challenge with re-creating the required trip geometry was reducing the width and thickness of the trip to match the reduction in chord of the rotor blade as a function of span. This was addressed by transitioning to fewer layers of tape over the span of the blade; however, the trip was still relatively large in chord compared to the trip used during 2D hydrofoil performance testing.



FIGURE 13. BOUNDARY LAYER TRIP

The application of the boundary layer trips had the dual effect of eliminating an unexpected reduction in thrust as a function of TSR as shown in blue line in Figure 14, but also slightly reducing the thrust of the rotor over the entire range of TSR as shown by the red line in Figure 14.

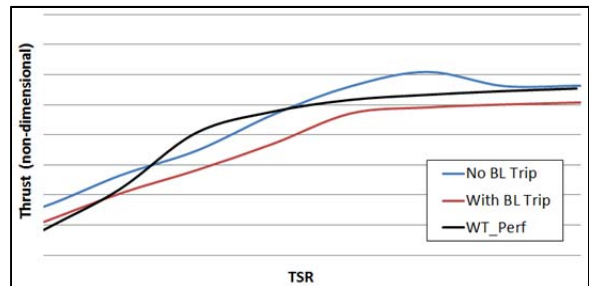


FIGURE 14. BOUNDARY LAYER TRIP IMPACT ON ROTOR THRUST

The reduction in thrust was compensated for by increasing blade pitch as described in the Performance and Loads Validation section.

Performance Validation

The model rotor was designed primarily to provide consistent thrust at very low Reynolds number rather than to optimize C_p . To achieve this design goal, some rotor efficiency was sacrificed. Tidal Bladed predicts a $C_{p_{max}}$ for the rotor of 0.41 for the un-coned model rotor. Analysis of test data shows a similar shape of the characteristic C_p -TSR curve, but a lower maximum value for $C_{p_{max}}$ of 0.38 as shown in Figure 15. This is due to the boundary layer trip being larger than what was represented in the pre-test numerical simulations. This value is also uncorrected for mechanical losses in the rotor

bearing and seal at the time of this publication. Future work may involve updating the numerical simulations to better match the test article; however, platform stability rather than power performance is the primary focus of this validation effort.

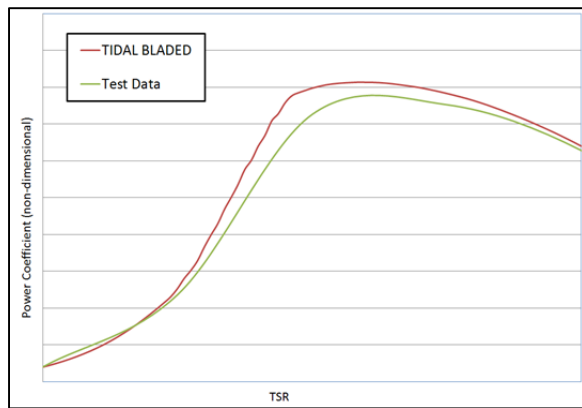


FIGURE 15. COMPARISON OF TIDAL BLADED POWER COEFFICIENT VERSUS TIP SPEED RATIO PREDICTIONS AGAINST TEST DATA AND WT_PERF

Loads Validation: Zero Yaw

Steady-state rotor thrust is the largest factor in the depth keeping of the C-Plane. Figure 16 shows variation of thrust with tip speed ratio. Several pitch angle settings were tested during tow tank testing and thrust variation with tip speed ratio are shown for a pitch angle of -1.6 and -2.6 degrees. Predictions from WT_PERF and Tidal Bladed are also plotted for comparison. At the design tip speed ratio, the measured thrust values are within 10% of the predictions. The observed deviation in thrust vs. TSR from predicted values is likely also attributable to the augmentation of foil performance due to the boundary layer trips used.

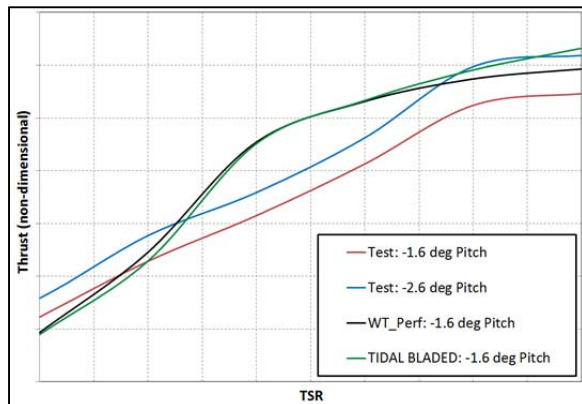


FIGURE 16. COMPARISON OF TIDAL BLADED THRUST VERSUS TIP SPEED RATIO PREDICTIONS AGAINST TEST DATA AND WT_PERF

Yawed Flow:

The next step was to compare loads predictions under yawed flow conditions. Data was collected for various yawed inflow conditions at the design tip speed ratio and current speed. This was done with the rotor configured both downstream and upstream of the support strut. Predictions of thrust from Tidal Bladed and FlightLab are within 10% of the test data for the upstream rotor configuration across the range of yaw angles as shown in Figure 17.

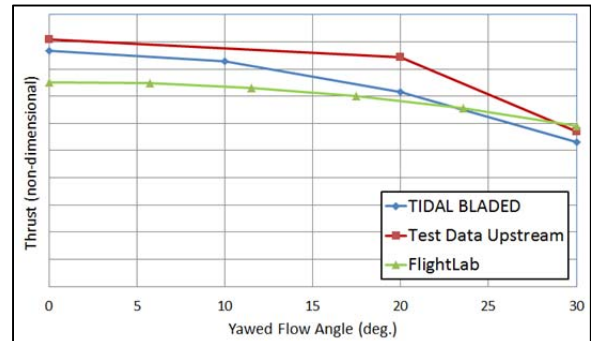


FIGURE 17. UPSTREAM COMPARISON OF TIDAL BLADED THRUST VERSUS YAW ANGLE PREDICTIONS AGAINST TEST DATA AND FLIGHTLAB

Figure 18 shows the variation of yaw moment at the load cell with yaw angle for the upstream rotor configuration. Tidal Bladed simulations match the measured yaw moment values within 20% at 30 degrees yaw and show identical trends of increasing yaw moment with increasing yaw angle.

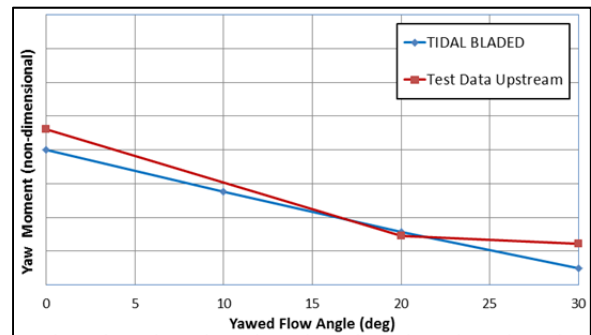


FIGURE 18. UPSTREAM COMPARISON OF TIDAL BLADED YAW MOMENT VERSUS YAW ANGLE PREDICTIONS AGAINST TEST DATA AND FLIGHTLAB

Figure 19 shows the variation of yaw moment at the load cell with yaw angle for the downstream rotor configuration. Simulations show similar trends of increasing yaw moment with increasing yaw angle, but almost half the magnitude. Possible causes of this discrepancy in magnitude include the strut wake (discussed later in the unsteady loads section) and load cell drift.

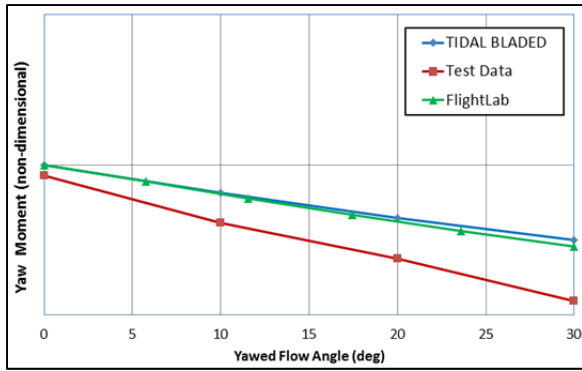


FIGURE 19. DOWNSTREAM COMPARISON OF TIDAL BLADED YAW MOMENT VERSUS YAW ANGLE PREDICTIONS AGAINST TEST DATA AND FLIGHTLAB

To better understand the discrepancy in yaw moment magnitude, the variation of thrust with yaw for the downstream rotor configuration is shown in Figure 20. This also shows an unexpected behavior where rotor thrust increases as the yaw angle increases. Both Tidal Bladed and FlightLab shows similar trends to the upstream data of reducing thrust with increasing yaw angle.

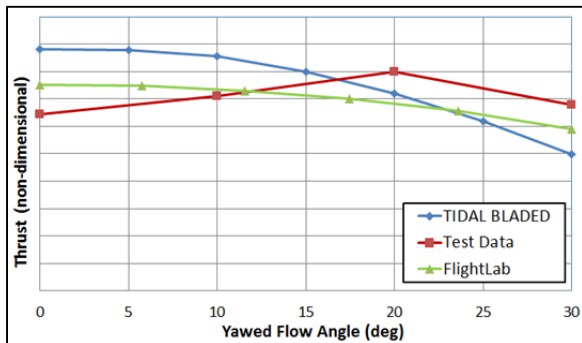


FIGURE 20. DOWNSTREAM COMPARISON OF TIDAL BLADED THRUST VERSUS YAW ANGLE PREDICTIONS AGAINST TEST DATA AND FLIGHTLAB

To investigate this unexpected thrust trend, a comparison of the C-Plane pitching moment at the load cell location for the downstream case is shown in Figure 21.

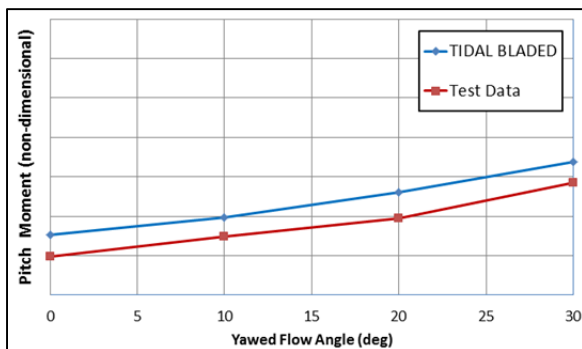


FIGURE 21. DOWNSTREAM COMPARISON OF TIDAL BLADED PITCH MOMENT VERSUS YAW ANGLE PREDICTIONS AGAINST TEST DATA

The trend of predicted pitching moment from Tidal Bladed is in agreement with test data. Since the mean pitching moment is a direct function of rotor thrust being applied at an offset distance from the load cell, the thrust test data plotted in Figure 20 is suspected to be in error due to an unknown problem with the data collection system. A related issue may also be affecting the yaw moment test data plotted in Figure 19.

Unsteady Loads: Yaw Moment

Investigations of the time-series yaw moment test data indicate high frequency content in the measurements. Figure 22 shows the 400Hz time-series yaw moment test data at 30 degrees flow angle for both upstream and downstream rotor configurations. This high frequency content is potentially due to support structure vibration, and may also be a contributing factor to the yaw moment discrepancy between the structurally rigid simulation predictions and the test data as shown in Figure 19. Also observed in the downstream yaw moment data is a spike at the minimum point in the oscillating signal. This is not found in the upstream data and may be the result of blade passage through the strut wake. This spike is one contributing factor to the increased downstream mean yaw moment values.

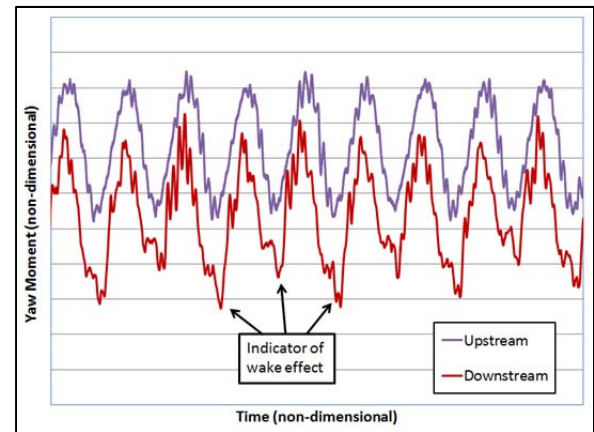


FIGURE 22. UPSTREAM VS. DOWNSTREAM YAW MOMENT TEST DATA AT 30 DEG FLOW ANGLE

DYNAMIC TEST

The primary goals of the dynamic test were to validate computational stability simulations, demonstrate steady-state loads avoidance techniques, determine behavior during all anticipated modes of operation and failure events, and reduce technical risk in key areas of the C-Plane design. Testing the complete device required a significantly more complex model, controller, and sensor package. One particularly challenging aspect was developing the Lab View controller to maintain rotor synchronization. This

controller allowed for the rotor to be accelerated or decelerated at specified rates while maintaining any specified phase relationship between the two rotors. Alternatively, the rotors could be run at different speeds in order to vary the thrust or torque differential between them in order to simulate a loss of torque control failure event.

Initial testing activities involved establishing the basic stability of the device and evaluating the pitch and depth response across a range of flow speeds. First, all sensors were zeroed and sensitivity studies were conducted. Secondly, the rotor thrust was balanced for synchronized rotors at the design speed to achieve near-zero yaw and sideslip using a trailing edge trim tab on the port rotor. The trim tab was used to achieve finer adjustment than was possible using the 1 degree blade pitch increments in the interchangeable hub inserts.

Speed sweeps at the design tip speed ratio correlate very well with predicted pitch and depth response as shown in Figure 23. The slight dip in C-Plane pitch just above the initial dive speed is likely due to an adjustment made to the restraint line on the umbilical cable. Despite the lack of vertical shear in the tow tank, this test did demonstrate the ability to seek a stable operating depth and so is very useful for continued development of the passive depth control loads avoidance technique in the simulated environment.

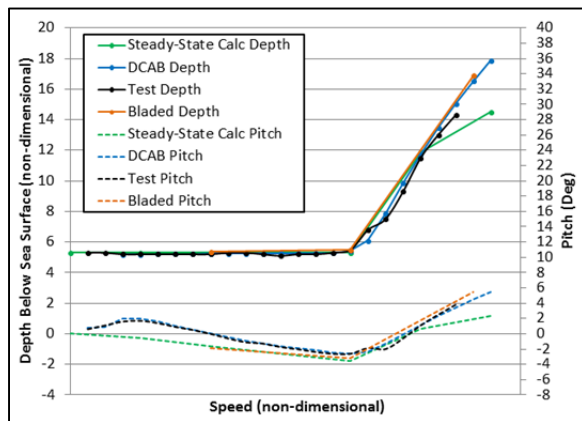


FIGURE 23. PITCH AND DEPTH RESPONSE

Yaw Validation

Testing included articulating the mooring anchor points up to -27.6deg with respect to the tow direction and collecting data over a range of speeds including reverse flow. Figure 24 shows the coordinate system for the yawed flow direction and C-Plane heading with respect to the mooring direction.

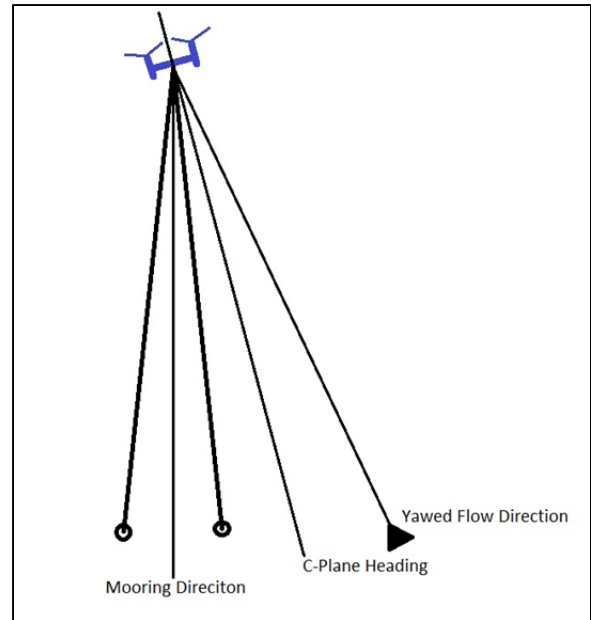


FIGURE 24. YAW RESPONSE TO FLOW DIRECTION

Figure 25 shows the DCAB prediction and measured yaw response of the C-Plane with respect to the moorings. During testing, the C-Plane remained within 5 degrees of each tested flow direction, and became better aligned as flow speed increases.

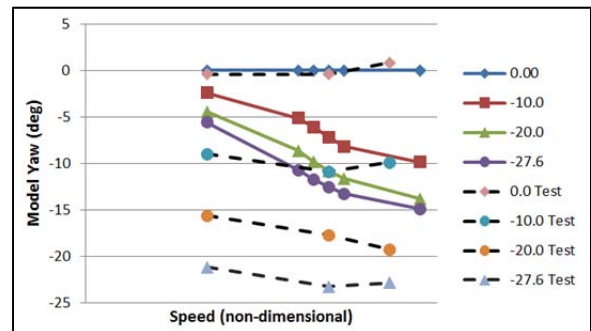


FIGURE 25. YAW RESPONSE TO FLOW DIRECTION

The discrepancy between the predicted yaw and test data is still being investigated; however, there is some variation in the measure yaw data as heading sensors primarily have to rely on inertial instruments due to magnetic disturbances from the basin and C-Plane electronics. Another potential cause of the discrepancies between simulation and measured yaw data is the use of a single forward mooring line in the DCAB simulation although dual lines were used on the test model as shown in Figure 24. A small lateral bridle (taking the form of a 4.6inch equilateral triangle) was also applied to the forward mooring lines during testing to bring the lines to the center of the transverse structure. This bridle was simulated in DCAB by implementing an equal length 'sting' strut that extended forward from the

center of the transverse structure with only a single degree of freedom in pitch.

Figure 26 shows the measured and DCAB predicted roll of the C-Plane over the same range of flow speeds and directions. During testing, the C-Plane was very roll stable - staying within 5 degrees of level regardless of flow direction. While DCAB predicts slightly more roll than measured, discrepancies are within 3deg.

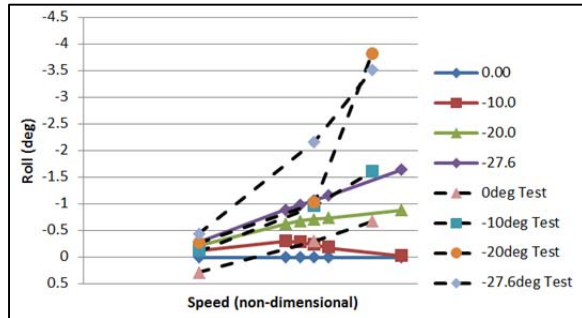


FIGURE 26. ROLL RESPONSE TO FLOW DIRECTION

CONCLUSIONS

Tow tank testing has shown the moored C-Plane design to be stable during all anticipated modes of operation over a wide range of flow conditions. The C-Plane has also demonstrated it has ample stability to safely react to a variety of failure modes including CG offsets resulting from asymmetric flooding, torque and thrust differentials resulting from asymmetric drivetrain failures, and others.

Although investigation of test results and tuning of simulation models continues, this effort has validated the ability of multiple simulation approaches to accurately predict the steady-state pitch and dive behavior of the C-Plane.

NEXT STEPS

A great deal of data was gathered during this testing effort which will help inform future design decisions of the C-Plane. Efforts continue to improve the accuracy of yaw and roll simulations. Transient cases such as start-up and shut-down are also being simulated. Some test cases still to be analyzed include the implementation of a wide forward mooring bridle to minimize transverse structure mass and wake, unsteady loading produced by the wake of upstream structures, and rotational stall delay on fixed pitch rotor blades.

Once the stability simulation validation using a model-to-model approach is complete, the next step will be to model the full-scale C-Plane in Tidal Bladed. This full scale model will be used to generate loads data for detailed component design. Tidal Bladed v4.4 has proven to be a very capable tool for modeling the moored C-Plane with its dual counter-rotating rotors. Further

Tidal Bladed software improvements currently underway include improved mooring representation, and the inclusion of lift and moment coefficients on non-rotating model components such as the C-Plane's transverse structure fairing.

ACKNOWLEDGEMENTS

The engineering and management team at Aquantis Inc. includes: Ole Kils, Tyler Mayer, Ken Gluck, Charles Vinick, Alex Fleming, and the author Henry Swales. The engineering and management team at the Naval Surface Warfare Center, Carderock Division includes: Richard Banko, Keith Brennan, Paul Strano, Kunal Patel, and contributing author David Coakley. Flightlab analysis of the C-Plane rotor was provided by Alan Schwartz, also from NSWCCD. The engineering team at DNV GL (Garrad Hassan) includes: William Collier and contributing author Stephen Way. Engineering and analysis expertise was also provided by contributing author Sandeep Gupta of Helios Engineering.

This effort was funded in part under a grant awarded to Dehlsen Associates by the U.S. Department of Energy.

REFERENCES

- (1) WT_Perf User Guide for Version 3.05.00 2012, National Renewable Energy Laboratory
- (2) Knutson, Richard and John Johnston, "A Three-Dimensional Dynamic Simulation for Submerged Cable Systems," CARDEROCKDIV-92/003 (April 1992).
- (3) Morton Gertler and Grant Hagen, "Standard Equations of Motion for Submarine Simulation", Naval Ship Research and Development Center (June 1967)
- (4) Tidal Bladed Theory Manual, Version 4.4. 2013, Garrad Hassan & Partners Ltd.
- (5) Way, S. et al. 2013 "Modeling A Floating, Multiple-Rotor Tidal Energy Converter Using Tidal Bladed", Proceedings of the 1st Marine Energy Technology Symposium